MECHANICAL PROPERTIES OF THE CELLULAR CYTOSKELETON

by **David H. Boal**
Dept. Of Physics, Simon Fraser University, Burnaby, BC V5A 1S6, Canada

I - INTRODUCTION

The human body contains about 10^{13} cells, whose size, shape and mechanical properties vary according to the capabilities of the cell:

Size: The typical length of a cell is measured in microns: a red blood cell is about eight microns in diameter, and many bacteria are about one micron in diameter and several microns in length. However, some cells, such as those transmitting signals from the brain to remote muscles, may be a metre in length. Further, there are compartments within cells as well as vesicles secreted by cells, which are typically several tenths of a micron in diameter.

Shape: Cell shapes span an amazing range from simple spheres to highly dendritic nerve cells. A cell's shape is not fixed for all time, if for no other reason than to accommodate growth. For example, a bacterium may elongate along its longitudinal axis and ultimately divide into two independent cells. The red blood cell must undergo strong deformation in its journey through the circulatory system, particularly as it passes through capillaries which may have a diameter less than half that of the blood cell. In some cases, a cell can travel along a surface by "willfully" changing its form, or can extend an arm in search of prey.

Elasticity: Cell shape is maintained, or changed, by several of its structural components. A bacterium may have an internal pressure of several atmospheres, and a multilayer network in the bacterial cell wall both resists this pressure, and yet permits the bacterium to grow. The red blood cell must have a shear resistance which is sufficiently small so that the cell can deform as it passes through a narrow capillary, yet is sufficiently large so that the cell can recover its rest shape after passage. Cells that can move on their own must have a dynamical internal structure that can actively change the cell's shape as required.

What components of the cell are responsible for maintaining its shape and/or providing its elasticity? Most bacteria, which are low on the evolutionary totem pole, have a multilayered network in their cell walls to resist rupture of the cell. More evolved cells, which during at least part of their lifetime contain internal compartments such as the cell's nucleus, have a *cytoskeleton* composed of a network of filamentous material. The cytoskeleton may be a full three-dimensional network, or, in the case of human red blood cells, a two-dimensional scaffolding attached to the plasma membrane that bounds the cell.

In general, Nature tends to be economical, if not outright parsimonious, in selecting the amount of materials needed for the structural components of a cell. For example, the one or more fluid sheets that make up the membrane encompassing the cell are about 5 nm thick, the principal components being dual chain lipid molecules arranged in the form of a bilayer. Yet, a lipid bilayer, fortified by cholesterol and sundry proteins, is both flexible enough to undergo strong deformations and robust enough to do so repeatedly; in the case of the human red blood cell, "repeatedly" means of the order 10^5 deformations in its 120-day lifetime. Similarly, the cytoskeleton and other structures in the cell are composed of biological chains, ropes and tubes having diameters of just 8 to 25 nm; yet, such networks can withstand pressures of up to many atmospheres, in some cases.

In Sec. II of this article, we introduce the reader to several generic components of the cell that are related to its mechanical properties. The operative word to describe most of these elements is *soft* although in no sense should this word be taken to mean *weak*. The mechanics of soft materials, being strongly influenced by thermal fluctuations in some cases, are not frequently covered in traditional undergraduate physics courses, and so a synopsis of some properties of soft materials, particularly isolated chains and sheets, is given in Sec. III. The chains are assembled into networks in Sec. IV, and used as an interpretive guide to biological networks. Finally, it is important to understand how networks fail: In biological systems failure of the cytoskeleton may be an undesirable phenomenon associated with disease, or it may be an action which we wish to encourage, such as the induced failure of the cell wall of an unwanted bacterium. Features of network failure are outlined in Sec. V.

There are far more aspects to the structure and function of the cell than will be presented in this article. The emphasis here is on the elastic properties of the cytoskeleton - in essence, its response to stress. Dynamical attributes of the cytoskeleton, such as how it provides a highway for the transportation of material within a cell, or how it dynamically rearranges to change the cell shape, are omitted. Further, the adhesion of cells to each other in a multicellular organism also is not discussed. An introduction to the many characteristics of the cytoskeleton not covered in this short review can be found in the general references which follow Sec. V.

The application of classical and statistical mechanics to biological systems is a young and rapidly evolving field of research. New experimental techniques continually increase our knowledge of biological structures and their response to stress. Our theoretical understanding of the static and dynamic properties of membranes has advanced substantially in the last decade. This article describes only a few of the many biological systems whose mechanical description either is available now or should be forthcoming in the near future.

II - STRINGS, TUBES AND SHEETS IN THE CELL

We begin with a few definitions from *lingua biologica*, a descriptive, elegant and vast language. In cells, a closed, simply-connected surface provides a membrane that segregates the cell's contents from its environment in a controlled way. Inside the surface resides the *cytoplasm*, which comprises the fluid *cytosol* and perhaps many smaller compartments called *organelles*; the region outside of the cell is referred to as the *extracellular space*. The *cytoskeleton* is a network of proteins that lies within the cytoplasm. The cytoskeleton may extend throughout the cytosol as a three-dimensional network, or may be a two-dimensional network attached to the cytoplasmic side of the cell boundary. Shown in Fig. 1 is the author's conception of the approximately triangular connectivity of the two-dimensional cytoskeleton in the human red blood cell.

Not all cells possess a network embedded in the cytosol. For example, a bacterium has no nucleus and no cytoskeleton, so

its internal structure is, in one sense, mechanically simple. Like plant cells, however, bacteria have a multilayer *cell wall* to resist the internal pressure of the cell. In Fig. 2, a cylinder with hemispherical caps represents a simple bacterium like *Escherichia coli*, a common bacterium of the intestinal tract. Note that the two-dimensional stress (force per unit length) on the cylinder's surface is anisotropic: the stress is *PR* in the ring around the cylinder, but *PR* / 2 along the axis of the cylinder, where *R* is the radius of the cylinder and *P* is the pressure difference across its surface. The skin of a hot dog under osmotic pressure (*i.e.*, overcooked) will tend to crack along its longitudinal axis, rather than break into two pieces (like a pair of sausages) because of this anisotropic stress.

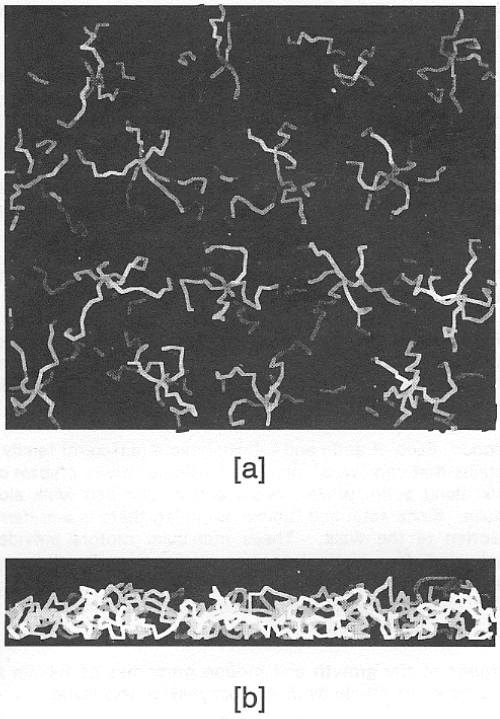

Fig. 1 **A computer model of the cytoskeleton attached to the envelope of the human red blood cell. The highly contorted strings joined together at six-fold junctions are tetramers of the protein *spectrin*. [a] Network seen from the cytoplasmic side of the membrane. [b] A section through the network. The lipid bilayer, a flat plane in this simulation, lies below the cytoskeleton in [b]. (From Boal, 1994).**

The bacterial cell wall has one of several forms, whose naming convention reflects their ability to retain Gram's stain. In *gram-positive* bacteria (*e.g.*, *Bacillus subtilis*), there is a single lipid bilayer, surrounded on the outside by many layers of peptidoglycan, the sugar/amino-acid network mentionned in Sec. I. In contrast, *gram-negative* bacteria (*e.g.*, *Escherichia coli*) have two lipid bilayers separated by a *periplasmic space* within which reside only a few layers of peptidoglycan. The envelopes of archaebacteria have no peptidoglycan. It should be emphasized that Figs. 1 and 2 are simplifications: there are other proteins embedded in the bilayer and these may extend into the cytoplasm, periplasm and extracellular space.

In summary, the structural elements of the cell are strings and tubes of proteins present in the cytoskeleton (for example) and two-dimensional sheets composed principally of dual chain lipids arranged in a bilayer. The molecular building blocks of the strings and tubes are amino acids, which are strung together to form proteins. Nature uses 20 amino acids in construction, each amino acid having both a carboxyl group (-COOH) and an amino group (-NH_2, except for proline, which has an NH group as a member of a ring). These amino acids are not particularly large, the smallest being glycine (NH_2 - CH_2 - COOH) with a molecular weight of 75 daltons. However, the molecular weight of a string of amino acids in the form of a protein molecule can easily surpass 10^5 daltons.

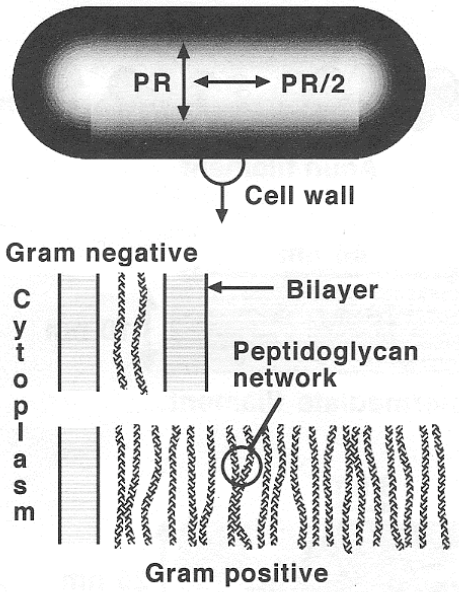

Fig. 2 **A schematic representation of a bacterium, which typically has a diameter of a micron. Seen in cross section, the bacterial cell wall contains a few (gram negative) or many (gram positive) layers of a *peptidoglycan* network whose chemical composition includes sugars and amino acids. Archaebacteria are exceptions to the rule, in that they have no peptidoglycan.**

The strings and tubes of the cytoskeleton are typically 8 to 25 nm in diameter, reflecting the way in which the proteins are linked together to form the filament. Two of the thinnest filaments are formed from the proteins spectrin and actin. *Spectrin* is a principal component of the cytoskeleton of the human red blood cell and auditory outer hair cells, to name two examples. In the simulated red cell cytoskeleton shown in Fig. 1, each chain represents a spectrin tetramer, which is

composed of two different kinds of spectrin monomers (molecular weights of ~220,000 and ~240,000 daltons). As shown schematically in Fig. 3, the spectrin monomers are probably intertwined to form the tetramer. The contour length along each monomer is about 100 nm, although the average displacement between the ends of the tetramer in the red cell is about 76 nm because of its contorted shape (Byers and Branton, 1985). Measured along the string, the mass per unit length is 4600 daltons/nm.

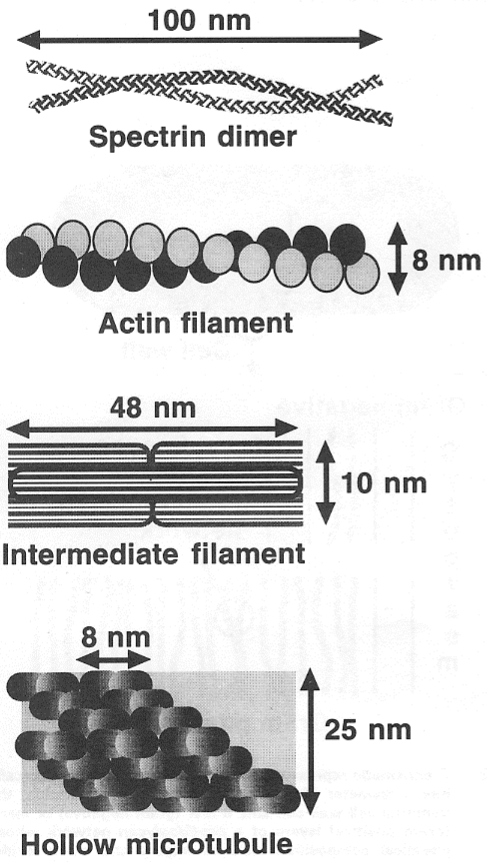

Fig. 3 Schematic representation of biological strings, ropes and tubes present in the cytoskeleton. The thinnest filaments include spectrin and F-actin, while the thickest are microtubules of tubulin. Between these extremes are the intermediate filaments.

Another flexible cytoskeletal string is *actin*, which is present in many different cell types and may play various roles in the cytoskeleton. The actin monomer is the protein G-actin (*G* for *globular*), which is a single chain of 375 amino acids having a molecular weight of 42,000 daltons. G-actin proteins can assemble to form a long string called F-actin (*F* for *filamentous*) as illustrated in Fig. 3. The mass per unit length along the filament is about 15,000 daltons/nm, a little more than 3 times that of spectrin. Correspondingly, the actin filaments appear stiffer than spectrin tetramers.

In contrast, the thickest filaments are hollow tubes of the protein *tubulin*. Molecular tubulin has two subunits (α-tubulin and β-tubulin), each of which has a molecular weight of about 100,000 daltons. The dimer of this globular protein can assemble into a hollow microtubule, which consists of 13 linear protofilaments. In each protofilament, the tubulin heterodimers are oriented α to β, as shown in Fig. 3. The overall molecular weight per unit length of microtubule is 160,000 daltons per nm, about ten times that of an actin filament, so that microtubules are relatively stiff. Their abundant number in nerve cells provides both strength and an internal transport system to long axons.

Between these two extremes lie the *intermediate filaments*, which can be formed from several varieties of proteins, and whose structure bears some resemblance to woven rope. The protein chains first form two dimers of coiled-coils, of length about 50 nm (represented by the single black cylinder in Fig. 3). Tetramers associate to form a rope of eight tetramers in cross section, 10 nm in diameter, with an alignment also shown in Fig. 3.

Although spectrin appears to play a rather passive role in the cytoskeleton, actin and tubulin filaments are dynamic:

•*Growth* Both actin and tubulin actively polymerize and depolymerize in a cell, so that the length of a string or tube is not static. The growth is not symmetric, in that the molecules, and hence the filaments, are polar.

•*Motion* Each of actin and tubulin have a (different) family of proteins that can "walk" along the string or tube. *Myosin* can walk along actin, while *kinesin* and *dynein* can walk along tubulin. Since actin and tubulin are polar, there is a preferred direction to the walk. These molecular motors provide a mechanism for protein ropes to glide past each other (*e.g.*, muscle cells) and for transport of chemicals within a cell (*e.g.*, nerve cells, in which neurotransmitter chemicals must be constantly replenished).

Features of the growth and motion properties of tubulin are explored in the article by J. A. Tuszynski in this issue.

The fluid membrane which bounds the cell is a self-assembled *lipid bilayer*. Although the phospholipids that make up the membrane have a heterogeneous composition, most of the lipids have two hydrocarbon chains typically with 14 to 18 methylene groups. The non-polar *hydrophobic* chains prefer their own company to that of water, while the polar headgroups of the phospholipid are *hydrophilic* and prefer to be surrounded by water molecules. Thus, in an aqueous environment, the polar head groups align as a two-dimensional sheet which hides the hydrocarbon chains from exposure to water. The situation is illustrated in Fig. 4, where both the exterior environment of the cell, and its cytoplasm, are aqueous. The assembly of *amphiphilic* molecules (such as lipids) into monolayers is discussed in the article by R. Desai in this issue.

None of the elements of the cytoskeleton attaches strongly to the lipid bilayer. Rather, there are attachment proteins that reside within the bilayer and provide the contact points for the

cytoskeleton. Some of these attachment points can be complex, involving several different proteins in association, as shown schematically in Fig. 4. Further, there are other proteins present in the cytoskeleton that crosslink different filaments, such as F-actin or microtubules.

The last structural element that we wish to introduce in this section is the peptidoglycan network which is found in almost all bacteria and whose chemical structure is illustrated in Fig. 5. Along the *x*-axis of the figure, there are a series of sugar rings which makes the network stiff in the *x*-direction. Transverse to this are chains of amino acids. Given that the average distance between the sugar chains is about 2 nm, the amino acids are not likely to be stretched out as dramatically as shown in the figure. Indeed, it has been found under some experimental conditions that the equilibrium area of the network may be only one third of the "stretched" area (see Koch, 1990). Of course, this doesn't mean that the chains are flopping around: there may be intra-chain interactions that cause the chains to fold up. Depending on the type of bacterium, there may be only a few or more than 20 layers of peptidoglycan. However, the word "layer" could be misleading, since there may be significant covalent bonding between adjacent glycan chains.

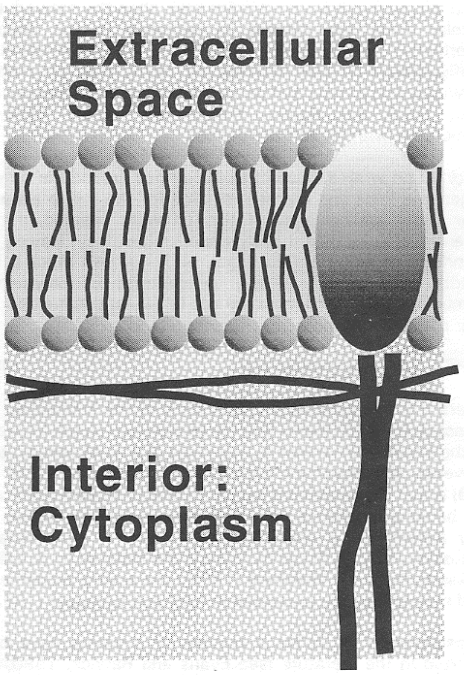

Fig. 4 **Lipid bilayers self-assemble from molecules that have hydrophobic acyl chains and hydrophilic polar headgroups. The cytoskeleton is attached to a lipid bilayer by a number of proteins, some of which are bound within the bilayer. The integral membrane proteins have hydrophobic segments that match the surrounding acyl chains of the lipids.**

III - FLEXIBLE CHAINS AND SHEETS

From Sec. II, we see that the principal components of the cytoskeleton or the bacterial cell wall are chains of varying stiffness, frequently crosslinked into a two- or three-dimensional net, and attached to a fluid sheet in the form of the lipid bilayer. In this section, we examine some fundamental properties of flexible chains and sheets, before moving on in Sec. IV to construct networks of chains and to use them to interpret biological systems.

Consider a simple model for a single polymer chain in which the polymer is a set of N vectors added tip-to-tail, each vector representing a bond or monomer. We assume here that each monomer has the same length a, and that the vector describing a particular monomer i is $\boldsymbol{a}_i$. The contour length, l_c, along the chain is then

$$l_c = Na, \qquad \text{(III.1)}$$

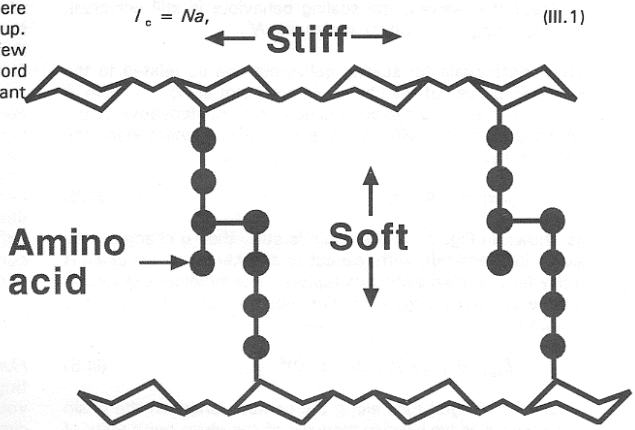

Fig. 5 **Structure of a single layer of the peptidoglycan network found in almost all bacteria. The network is stiff along the axis containing the sugar rings, and soft in the direction of the amino acid chains. (After Koch, 1990).**

and, as shown in Fig. 6, the end-to-end displacement, $\boldsymbol{r}_{ee}$, is just the sum of the individual vectors, $\boldsymbol{a}_i$:

$$\boldsymbol{r}_{ee} = \Sigma_i \boldsymbol{a}_i. \qquad \text{(III.2)}$$

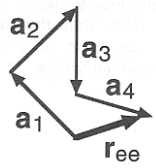

Fig. 6 **End-to-end displacement, $\boldsymbol{r}_{ee}$, for a chain whose elements have a common length and random orientation.**

Taking the ensemble average over all chains with the same number of monomers, N, the end-to-end displacement squared, $\langle r_{ee}^2 \rangle$, is

$$\langle r_{ee}^2 \rangle = \Sigma_i \Sigma_j \langle \boldsymbol{a}_i \cdot \boldsymbol{a}_j \rangle. \qquad \text{(III.3)}$$

If a given bond vector $\boldsymbol{a}_i$ can have any orientation independent of any other vector $\boldsymbol{a}_j$, then the ensemble average of $\boldsymbol{a}_i \bullet \boldsymbol{a}_j$ should vanish if $i \neq j$. Thus, the only terms which survive in the double sum in Eq. (III.3) are the diagonal elements $i = j$, each of which equal a^2. For a freely jointed chain, then

$$\langle r_{ee}^2 \rangle = Na^2. \qquad \text{(III.4)}$$

Suppose that the chain were not freely jointed, but nevertheless could intersect itself; an example would be a chain in which neighbouring elements have a fixed polar angle (like C-C-C bonds in an alkane chain) but are free to rotate azimuthally. Even here, one finds that $\langle r_{ee}^2 \rangle = Nb^2$, although the length scale b is longer than that of the C-C bond (see Flory, 1953). The scaling behaviour $\langle r_{ee}^2 \rangle \sim N^1$ in Eq. (III.4) is referred to as ideal scaling, and it applies to linear chains that can intersect themselves. Note that, even if the chains are *not* allowed to intersect themselves, the scaling behaviour is still universal, although $\langle r_{ee}^2 \rangle$ no longer scales like N^1.

The length scale for scaling behaviour can be related to the elastic properties of the chain. At any point along the chain, a unit tangent vector $\boldsymbol{u}$ can be obtained from the derivative of the coordinate position, $\boldsymbol{R}(s)$, with respect to the length along the chain, s, by:

$$\boldsymbol{u}(s) = \partial \boldsymbol{R} / \partial s, \qquad \text{(III.5)}$$

as shown in Fig. 7. If the chain is stiff, then $\boldsymbol{u}$ changes only slowly in orientation with respect to s; whereas, if the chain is highly flexible, then $\boldsymbol{u}$ changes rapidly. The simplest expression for the bending energy of a continuous, flexible chain has the quadratic form,

$$E_{bend} = (Y_b / 2) \int ds \, (\partial \boldsymbol{u} / \partial s)^2 \qquad \text{(III.6)}$$

where the integral runs along the contour length of the chain and where Y_b is the bending modulus of the chain (with units of energy per unit length). For a chain described by Eq. (III.6), the orientation of the unit tangent vector becomes decorrelated according to (see Doi and Edwards, 1986)

$$\langle \boldsymbol{u}(s) \bullet \boldsymbol{u}(0) \rangle = \exp(-s / \xi_p), \qquad \text{(III.7)}$$

where ξ_p is the persistence length. In terms of the bending parameter, Y_b, the persistence length is

$$\xi_p = bY_b \qquad \text{(III.8)}$$

where b is the inverse temperature $(k_B T)^{-1}$ with k_B representing Boltzmann's constant. Note that the persistence length is temperature-dependent, as one might expect: at low temperature, the persistence length tends to infinity.

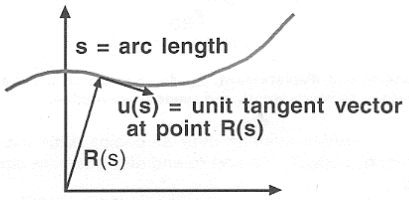

Fig. 7 **Relation between unit tangent vector, u, and position of point, R, on a curve.**

For alkanes, the persistence lengths are in the range of 0.2 nm, which is roughly the length of a covalent bond. Protein chains, in contrast, have much longer persistence lengths; for example, the persistence length of spectrin is 10 - 20 nm (see Stokke *et al.* 1985; Svoboda *et al.*, 1992). DNA has a still longer persistence length, at 50-55 nm (Taylor and Hagerman, 1990; Bustamante *et al.*, 1994). From Eq. (III.8), the ordering of increasing bending resistance is: alkanes, spectrin, DNA.

The concept of persistence length can be applied to sheets as well, by replacing in Eq. (III.7) the tangent vector $\boldsymbol{u}$ from chains with the unit vector $\boldsymbol{n}$ normal to the surface. The linear bending modulus, Y_b, can be generalized to a surface bending resistance, k_b, which has units of energy (see Deuling and Helfrich, 1976). The expression for the bending energy of a surface in terms of k_b and the principal curvatures of the surface, requires more explanation than we have space for in this article, so we provide only the following observations as intuition for how the persistence length depends on k_b. The behaviour depends upon the nature of the membrane connectivity - whether it is polymerized or fluid.

Polymerized: Suppose that we were to take a set of highly flexible rods and weave them together in a two-dimensional fabric, welding fixed cross-links wherever the rods cross each other. We refer to this as a polymerized network. If we try to bend this network in an arbitrary way, then the network may develop folds and creases in response to the imposed deformation. The formation of folds and creases restricts the configurations of the network so much that polymerized networks are, in fact, flat on long length scales (Plischke and Boal, 1988; see Kantor, Kardar and Nelson, 1986 for membranes without self-avoidance).

Fluid: If you wrap a piece of aluminum foil around the tip your finger, the folds and creases required for the foil to adapt to your finger are obvious. If the foil were, instead, a two-dimensional fluid, then the folds could relax away, leaving just a uniform coating on your finger, as if you had stuck it into (cold!) cooking oil. Thus, in contrast to polymerized membranes, fluid membranes are not flat at long distances, and their persistence length is approximately

$$\xi_p \sim a \exp(-4\pi\beta k_b / 3) \qquad \text{(III.9)}$$

where a is an elementary length scale of the membrane. As expected, Eq. (III.9) shows that the persistence length increases as the bending resistance k_b increases at a fixed temperature. However, the important difference between Eqs. (III.8) and (III.9) is that the persistence length increases *exponentially* with the bending resistance for a two-dimensional membrane, but only *linearly* for a one-dimensional rod. A more detailed discussion of Eq. (III.9) can be found in the lectures by S. Leibler in Nelson, Piran and Weinberg (1989); the scaling properties of fluid membranes are presented in Kroll and Gompper (1992).

Measurements of k_b for a number of systems have been reported in the literature (see Evans and Rawicz, 1990, and references therein). Single-component bilayers composed of the types of lipids found in cells typically have bending moduli of the order $(0.4 - 1) \times 10^{-19}$ J, which is 10-25 $k_B T$ at room temperature. Adding cholesterol to the bilayer at concentrations found in red blood cells significantly increases the bending modulus. With a bending modulus $k_b = 10\, k_B T$ and an elementary length scale $a = 1$ nm, Eq. (III.9) gives an estimated bilayer persistence length of 10^9 m. In spite of its impressive size, this number should be interpreted only as

indicating that undulations in a bilayer are smooth, but not absent, on the length scale of hundreds of nanometres.

IV - NETWORK ELASTICITY

Elastic moduli have been measured for both two- and three-dimensional protein networks, as we present in more detail later in this section. Compared to conventional solids or liquids, the moduli are found be *very* small, reflecting the fact that protein networks in cells have a low density of network junctions. To provide a framework for interpreting the measurements, we examine the moduli of two simple systems: an ideal gas and a two-dimensional network of chains.

Ideal gas: The equation of state of an ideal gas held at a pressure P has the well-known form $PV = Nk_BT$, where N is the number of particles contained in the volume V. The ideal gas has a vanishing shear modulus, but has a non-zero volume compression modulus, K_V, which can be obtained from the change in volume as a function of pressure:

$$K_V^{-1} = -V^{-1} (\partial V / \partial P). \qquad \text{(IV.1)}$$

Substituting the equation of state into Eq. (IV.1), the compression modulus for an ideal gas is found to be equal to its pressure, $K_V = P$, or equivalently,

$$K_V = \rho k_B T, \qquad \text{(IV.2)}$$

where ρ is the density of particles, N/V. The area compression modulus K_A for a two-dimensional ideal gas has a similar expression, with the density ρ becoming the number of particles per unit area, N/A.

Chain network in two dimensions: Eq. (III.8), shows that the persistence length of a flexible chain decreases with temperature: in other words, the chain shrinks with increasing temperature. This effect is easy to demonstrate by heating a rubber band with a hair-dryer. In turn, this implies that energy must be added to a chain to stretch it, even if the internal energy of the links in the chain is unchanged: flexible materials are elastic by virtue of their entropy. The force required to change the end-to-end displacement of a flexible chain is proportional to the displacement from equilibrium, just as in Hooke's Law, with a spring constant given by

$$k_{sp} = dk_BT / Na^2, \qquad \text{(IV.3)}$$

where d is the dimension in which the spring is embedded and the other symbols are defined in Eq. (III.4) (for further reading, see de Gennes, 1979).

A network of flexible chains is also elastic. Consider the triangulated spring network in two dimensions shown in Fig. 8. The elastic moduli can be extracted by subjecting the spring network to a set of known deformations and evaluating the change in potential energy. At zero temperature, one finds

$$K_A = \sqrt{3}\, k_{sp} / 2 \qquad \text{(IV.4)}$$

and

$$\mu = \sqrt{3}\, k_{sp} / 4, \qquad \text{(IV.5)}$$

where k_{sp} is the spring constant (see Boal, Seifert and Shillcock, 1993).

Eq. (IV.3) approximates the effective spring constant of a chain in a network, so that two-dimensional networks of chains should have elastic moduli of the order k_BT / Na^2, according to Eqs. (IV.4) - (IV.5). Replacing Na^2 with $\langle r_{ee}^2 \rangle$ [Eq. (III.4) for ideal chains] and noting that the density of network junctions, ρ, is $\langle r_{ee}^2 \rangle^{-1}$ to within factors of two, then the elastic moduli should be roughly

$$\mu \sim K_A \sim \rho k_BT, \qquad \text{(IV.6)}$$

similar to the ideal gas expression. Admittedly, this derivation is a little crude, but simulations of self-avoiding chains show that it is accurate to within an order of magnitude (see also Chap. XI of Flory, 1953).

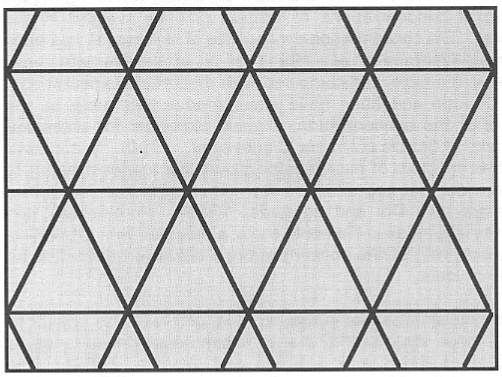

Fig. 8 At zero temperature, a triangular network of springs in two dimensions has a compression modulus of $\sqrt{3}\, k_{sp} / 2$ and a shear modulus of $\sqrt{3}\, k_{sp} / 4$, where k_{sp} is the spring constant.

A commonly-used experimental technique for determining the elastic properties of cells has been to subject the cell to a known stress and then to analyse the resulting strain to obtain the elastic moduli. Because of their simple internal structure, red blood cells have been studied extensively; results for cells from a number of species are given in Table IV.1. It should be noted that a different technique, which measures long wavelength fluctuation of a cell surface, gives a lower value for the shear modulus of human red blood cells. The most recent measurements investigate the red cell cytoskeleton under both extension and compression (Discher *et al.*, 1994).

Table IV.1 Shear moduli of red blood cells as measured by micromechanical manipulation (Waugh and Evans, 1979).

Species	Modulus	Experiment (N/m)
Human	2D Shear	$6\text{-}9 \times 10^{-6}$
Opossum	2D Shear	8×10^{-6}
Turkey	2D Shear	4×10^{-5}
Conga snake	2D Shear	7×10^{-5}
Painted turtle	2D Shear	10×10^{-5}

The magnitudes of the moduli are modest. The reason for the small values is that the cytoskeletons of blood cells are fairly loose, as one can see from the simulation shown in Fig. 1. It

was suggested by Evans (1973) that the elastic properties of the red cell cytoskeleton could be understood in terms of polymer elasticity. If one uses the known density of network junctions in the human red blood cell, then Eq. (IV.6) predicts that the elastic moduli should be of the order 10^{-6} N/m. Considering the approximations involved in obtaining Eq. (IV.6), this result is surprisingly close to the measured value. A detailed simulation which includes steric interactions among cytoskeleton elements *etc*. confirms that the shear modulus expected within a polymer chain model for the human red blood cell should be close to 10^{-5} N/m (Boal, 1994).

Measurements also have been made of the shear modulus of isolated components of the cytoskeleton, and results for actin, fibrin, vimentin and microtubules are shown in Table IV.2 (from Janmey *et al.*, 1991). For comparison, typical compression moduli are shown for a liquid and an ideal gas at STP, although the shear moduli of these fluids vanish. The moduli for the protein networks shown in the table are small, reflecting in part the small concentrations of protein (2% by weight) in the samples. The concentration-dependence of the moduli has been reported (Janmey *et al.*, 1991) for all of the filament types shown in the table, and compared with theoretical expectations. Both F-actin and fibrin have shear moduli that grow as the square of the concentration, a result expected for entangled networks of flexible polymers (Clarke *et al.*, 1990). In contrast, the shear modulus of microtubules grows like $[concentration]^{1.3}$, a behaviour not too different from that expected for rodlike polymers (see Doi and Edwards, 1986). Perplexingly, the vimentin intermediate filaments show a modulus that grows like the square root of the concentration, a result not described by simple models.

Peptidoglycan networks in the bacterial cell wall also appear to have a loose structure, in that they can be stretched by up to a factor of three in area (Koch and Woeste, 1992). The mechanical characteristics of peptidoglycan are currently under active investigation. Recent measurements the elastic properties of the sheath that surrounds cells of the archaeobacterium *Methanospirillum hungatei* yield a Young's modulus of $(2\text{-}4)\cdot 10^{10}$ N/m^2 (Xu *et al.*, 1997). This modulus is relatively large, and suggests that the sheath can withstand pressures of hundreds of atmospheres.

Table IV.2: Elastic moduli of three-dimensional networks at 2 mg/ml (Janmey *et al.*, 1991). Fibrin is a protein that holds blood clots together, while vimentin is an intermediate filament.

System	Modulus	Experiment (atmospheres)
Typical liquid	3D volume	10^4
Ideal gas at STP	3D volume	1
Actin	3D shear	2.8×10^{-3}
Fibrin	3D shear	1.0×10^{-3}
Vimentin	3D shear	3.2×10^{-4}
Microtubules	3D shear	3.4×10^{-4}

V - NETWORK FAILURE

Nature rarely provides us with networks whose connectivity is as regular as that shown in Fig. 8. In fact, uniform connectivity may not be needed, nor even helpful, for the functioning of the network in a cell. However, if the connectivity of a network is too low (*i.e.*, too few bonds per junction), then the network may fail. For example, if the amount of spectrin protein in a red blood cell is too low, then the cytoskeleton elasticity may not be large enough for the cell to perform its function (for a review, see Mohandas and Evans, 1994). Thus, it is important to understand the properties of depleted and irregular networks, as well as regular ones. This takes us into the study of *percolation*.

Consider the two-dimensional square lattices in Fig. 9, in which bonds have been placed between lattice sites in a random fashion. The population of bonds on the lattice as a whole can be described by a parameter p, which is the probability that a given bond site is occupied. If the lattice has a full complement of bonds, then $p = 1$ and each site on the lattice has four-fold connectivity. If no bonds are present, then obviously $p = 0$. The two example configurations in the figure have values of p intermediate between 0 and 1.

One attribute of a configuration is whether a continuously connected path traverses the lattice. Such a path is absent in configuration [a] of Fig. 9 (with $p = 1/3$), but present in configuration [b] (with $p = 2/3$). For infinite systems, the existence of a connecting path across the lattice is a discontinuous function of p and there is a well-defined value of p, called the connectivity percolation threshold p_C, below which there is no connecting path. The connectivity threshold is lattice-dependent: in two dimensions, $p_C = 0.5$ for a square lattice and $p_C \approx 0.35$ for a triangular lattice. The two values of p shown for a small square lattice in Fig. 9 bracket the connectivity threshold.

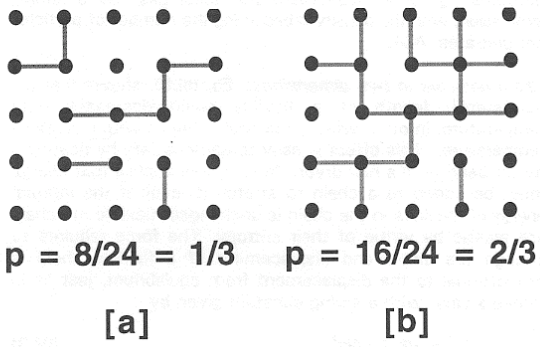

Fig. 9 Percolation phenomena on a square lattice in two dimensions. Configuration [a], with bond occupation probability $p = 1/3$, is below the connectivity percolation threshold, while configuration [b], with $p = 2/3$, is above the connectivity threshold. In this particular example, no bonds are placed along the edge of the lattice, so the maximum allowable number of bonds is 24.

The elastic moduli also depend upon p: for $p < p_C$, the network is not connected and can support neither shear nor compression, so that both μ and K_A vanish. However, the presence of a connecting path at $p > p_C$ does not guarantee that the network can resist deformation. Even though p is safely above p_C in configuration [b], there is only one connecting path from left to right - which is not a lot of paths to resist shear. It is found (Feng and Sen, 1984) that the resistance to compression or shear vanishes below a distinct threshold, referred to as the rigidity percolation threshold p_R. In general, p_R is larger than p_C: in numerical studies of triangular networks, $p_R \approx d\,p_C$, where d is the embedding dimension of the network (Feng, Thorpe and Garboczi, 1985).

Once the percolation thresholds have been crossed from below, the elastic moduli do not rise immediately to their values for a fully connected network with $p = 1$. Rather, to a first approximation, they rise linearly with p for p not too close to p_R. For example, the shear modulus is described approximately by

$$\mu(p) / \mu(p=1) \sim (p - p_R) / (1 - p_R) \quad \text{for } p \gg p_R$$
$$\mu(p) = 0 \quad \text{for } p < p_R, \qquad \text{(V.1)}$$

as shown in Fig. 10 (Note that the value of p_R obtained by fitting the linear regime of $\mu(p)$ with Eq. (V.1) is inaccurate by a few percent). Further discussion of the elastic properties of networks with random cross links can be found in the article by M. Plischke in this issue.

As stated at the beginning of this section, there are numerous examples of cytoskeletons with irregular or reduced connectivity. Examples of such two-dimensional networks are the spectrin-depleted cytoskeletons of red blood cells found in some individuals with a specific hereditary blood disorder (Waugh and Agre, 1988). In these cells, the main component of the cytoskeleton (spectrin) is observed to be reduced below the normal value, and the shear modulus of these cells is correspondingly lower. The range of the data is shown in Fig. 10, where it is seen that the measured values of $\mu(p) / \mu(p=1)$ do decrease roughly linearly with p, but not to the degree expected from percolation theory. This does not necessarily mean that percolation theory is inapplicable to spectrin-depleted blood cells; it may be that the coordination of such cytoskeletons is still relatively uniform, although less than six-fold.

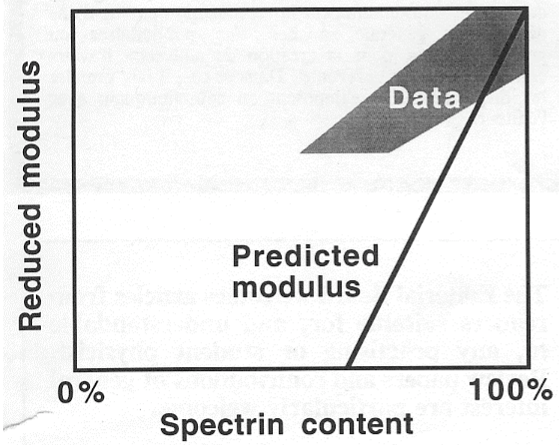

Fig. 10 **Schematic representation of the reduced shear modulus (μ / μ_1) as a function of bond occupation probability p at zero temperature. The subscript 1 refers to the value of the modulus at $p = 1$ (all bonds occupied). Both the shear and compression moduli vanish at the rigidity percolation threshold, p_R, which is larger than the connectivity percolation threshold, p_c. (The behaviour of $\mu(p)$ close to $p = p_R$ is more subtle than the simple linear form shown). Displayed for comparison is the range of experimental measurements of the shear modulus for spectrin-depleted human red blood cells.**

ACKNOWLEDGMENTS

The author wishes to thank Michael Wortis and Evan Evans for introducing him to the fascinating subject of biophysics. The annual meeting of the Soft Surfaces and Interfaces Program of CIAR, directed by Myer Bloom, has strongly influenced the author's research program, as has Michael Plischke, with whom he wrote his first paper in statistical mechanics. The author has benefitted from collaboration with several former students and postdoctoral fellows at Simon Fraser University, including Udo Seifert, Madan Rao, Julian Shillcock, Tony Boey and Dennis Discher; space does not permit the presentation of all of their results. This work is supported in part by the Natural Sciences and Engineering Research Council of Canada.

REFERENCES

The cell

B. Alberts, D. Bray, J. Lewis, M. Raff, K. Roberts and J. D. Watson, 1989. *Molecular Biology of the Cell*, second ed. (Garland, New York), Chap. 11.

The cytoskeleton and its components

J. E. Hesketh and I. F. Prym, eds., 1996. *The Cytoskeleton*, Vol. 2, Role in Cell Physiology (JAI Press, Greenwich, Conn.).

J. S. Hyams and C. W. Lloyd, eds., 1994. *Microtubules* (Wiley-Liss, New York).

D. A. D. Parry and P. M. Steinert, 1995. *Intermediate Filament Structure* (Landes, Austin, Tx.), Chaps. 1-3.

T. M. Preston, C. A. King and J. S. Hyams, 1990. *The Cytoskeleton and Cell Motility* (Blackie, Glasgow), Chaps. 2-3.

Polymers and Sheets

P.-G. de Gennes, 1979. *Scaling Concepts in Polymer Physics* (Cornell University Press, Ithaca).

D. Nelson, T. Piran and S. Weinberg, eds., 1989. *Statistical Mechanics of Surfaces and Interfaces* (World Scientific, Singapore).

S. A. Safran, 1994. *Statistical Thermodynamics of Surfaces, Interfaces and Membranes* (Addison-Wesley, New York).

Work cited

D. H. Boal, 1994. Computer simulation of a model network for the erythrocyte cytoskeleton. *Biophys. J.* 67:521-529.

D. H. Boal, U. Seifert and J. C. Shillcock, 1993. Negative Poisson ratio in two-dimensional networks under tension. *Phys. Rev.* E48:4274-4283.

C. Bustamante, J. F. Marko and E. D. Siggia. 1994. Entropic elasticity of λ-phage DNA. *Science* 265:1599-1600.

T. J. Byers and D. Branton. 1985. Visualizations of the protein associations in the erythrocyte membrane skeleton. *Proc. Natl. Acad. Sci. USA* 82:6153-6157.

A. Clarke, S. Ross-Murphy, K. Nishinari and M. Watase. 1990. Shear modulus-concentration relationships for biopolymer gels. Comparison of independent and cooperative crosslink descriptions. *In* Physical Networks: Polymers and Gels. W. Burchard and S. Ross-Murphy, eds. (Elsevier, London).

D. E. Discher, N. Mohandas and E. A. Evans. 1994. Molecular maps of red cell deformation: hidden elasticity and *in situ* connectivity. *Science* 266:1032-1035.

M. Doi and S. F. Edwards. 1986. *The Theory of Polymer Dynamics* (Oxford University Press), pgs. 316-318.

H. J. Deuling and W. Helfrich. 1976. The curvature elasticity of fluid membranes: a catalogue of vesicle shapes. *J. Physique* 37:1335-1345.

E. A. Evans. 1973. New membrane concept applied to the analysis of fluid shear- and micropipette-deformed red blood cells. *Biophys. J.* 13:941-954.

E. A. Evans and W. Rawicz. 1990. Entropy-driven tension and bending elasticity in condensed-fluid membranes. *Phys. Rev. Lett.* 64:2094-2097.

S. Feng and P. N. Sen. 1984. Percolation on elastic networks: new exponent and threshold. *Phys. Rev. Lett.* 52:216-219.

S. Feng, M. F. Thorpe and E. Garboczi. 1985. Effective-medium theory of percolation on central-force elastic networks. *Phys. Rev. B* 31:276-280.

P. J. Flory. 1953. *Principles of Polymer Chemistry* (Cornell University Press, Ithaca), Chap. X.

P. A. Janmey, U. Euteneuer, P. Traub and M. Schliwa. 1991. Viscoelastic properties of vimentin compared with other filamentous biopolymer networks. *J. Cell Biol.* 113:155-159.

Y. Kantor, M. Kardar and D. R. Nelson. 1986. Statistical mechanics of tethered surfaces. *Phys. Rev. Lett.* 57:791-794.

A. L. Koch, 1990. Growth and form of the bacterial cell wall. *Amer. Scientist* 72:327-341.

A. L. Koch and S. Woeste. 1992. Elasticity of the sacculus of *Escherichia coli*. *J. Bacter.* 174:4811-4819.

D. M. Kroll and G. Gompper. 1992. The conformation of fluid membranes: Monte Carlo simulations. *Science* 255:968-971.

N. Mohandas and E. A. Evans. 1994. Mechanical properties of the red cell membrane in relation to molecular structure and genetic defects. *Annu. Rev. Biophys. Biomol. Struct.* 23:787-818.

M. Plischke and D. H. Boal. 1988. Absence of a crumpling transition in strongly self-avoiding tethered membranes. *Phys. Rev.* A38:4943-4945.

B. T. Stokke, A. Mikkelsen and A. Elgsaeter. 1985. Human erythrocyte spectrin dimer intrinsic viscosity: temperature dependence and implications for the molecular basis of the membrane free energy. *Biochim. Biophys. Acta* 816:102-110.

K. Svoboda, C. F. Schmidt, D. Branton and S. M. Block. 1992. Conformation and elasticity of the isolated red blood cell membrane skeleton. *Biophys. J.* 63:784-793.

W. H. Taylor, and P. J. Hagerman. 1990. Application of the method of phage T4 DNA ligase-catalysed ring-closure to the study of DNA structure. II NaCl-dependence of DNA flexibility and helical repeat. *J. Mol. Biol.* 212:363-376.

R. E. Waugh and P. Agre. 1988. Reductions of erythrocyte membrane viscoelastic coefficients reflect spectrin deficiencies in hereditary spherocytosis. *J. Clin. Invest.* 81:133-141.

R. Waugh and E. A. Evans, 1979. Thermoelasticity of red blood cell membrane. *Biophys. J.* 26:115-132.

W. Xu, P. J. Mulhern, B. L. Blackford, M. H. Jericho, M. Firtel and T. J. Beveridge. 1997. Modelling and measuring the elastic properties of an archeal surface, the sheath of *Methanospirillum hungatei*, and the implication for methane production. *In press*.

The Editorial Board welcomes articles from readers suitable for, and understandable to, any practising or student physicist. Review papers and contributions of general interest are particularly welcome.

Le comité de rédaction invite les lecteurs à soumettre des articles qui interessaient et seraient compris par tout physicien, ou physicienne, et étudiant ou étudiante en physique. Les articles de synthèse et d'intérêt général sont en particulier bienvenus.